the layer for $2\theta < 51.2^{\circ}$ (for Cu K_{α}), resulting in about 3500 data points and a total collection time of about 1 week. Counting time was chosen after some initial tests to achieve average counting errors in the intensity measurements of better than 10%. In all, data for 6 reciprocal lattice sections have been collected, and a detailed comparison with corresponding photographic data will be described.

An example contour plot, illustrating the quality of data obtained is shown in Figure 1.

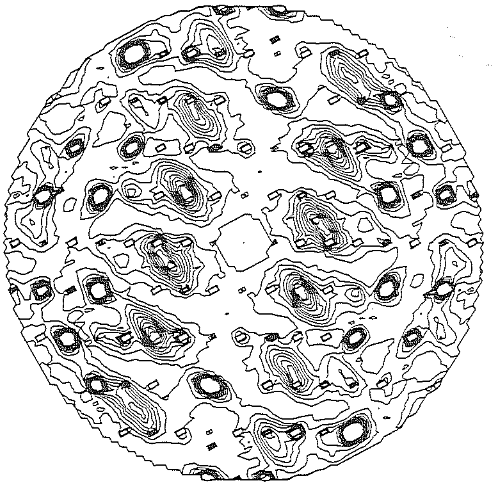

Figure 1. Contour plot of the h0l data. Contour levels are in equal increments of 250 counts. Bragg peaks appear as small quadrilaterals.

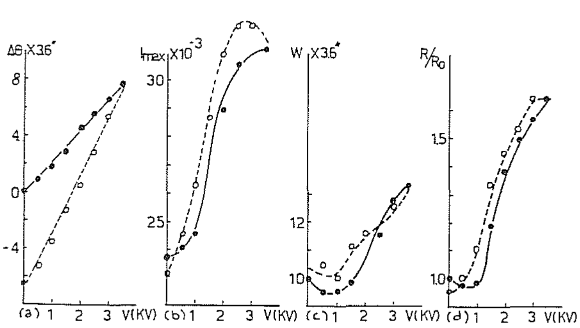

Fig. 1 Dependence of (a) peak shift, (b) maximum intensity, (c) half-width and (d) percentage integrated intensity on the applied DC voltage ((203) reflection, thickness of crystal t=0.31 mm, irradiated face at positive potential).
• increasing field; o decreasing field

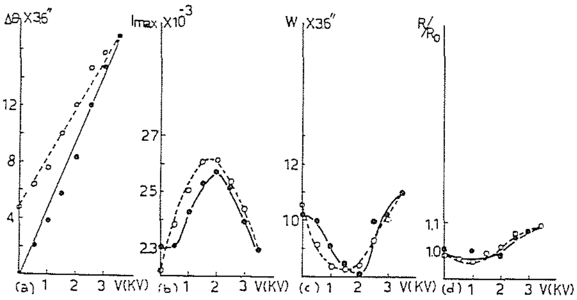

Fig. 2 Same as fig. 1 with reversed polarity.

11.5–4 EFFECTS OF ELECTROSTATIC FIELD ON THE X-RAY BRAGG DIFFRACTION OF α-QUARTZ.

By M. Calamiotou, Physics Dept., Athens Univ., E. Anastassakis, National Technical Univ., Athens, V. Psicharis and S.E. Filippakis, N.R.C. "Demokritos", Athens.

An increase of the X- and γ-ray integrated intensity of α-Quartz under the influence of an electrostatic field has been observed by Yasuda and Kato (Appl. Cryst.(1975) 8, 623) and Dousse and Kern (Acta Cryst. (1980) A36, 966) respectively, but the mechanism responsible for such an effect is not yet completely clear. We report here the results of an experimental study, in which a series of rocking curves of the (203) X-ray Bragg reflection of α-Quartz were measured in the presence of an electrostatic field up to ∿113 kV/cm. The integrated intensity at constant field was found to be time-dependent, suggesting the existence of relaxation effects. A field-dependent saturation value was reached after time intervals ranging from 20 to 45 min for field values of 16 to 113 kV/cm. Rocking curve characteristics such as peak position, peak intensity and half width were measured as a function of the field at saturation level (fig. 1a,b,c and d for percentage change of the integrated intensity). They all show hysteresis effects. It was also observed that the strength of the effect depends on the field polarity. When the negative electrode was attached to the irradiated face the effects were considerably reduced (fig. 2a,b,c,d). The measured peak shifts Δθ are typically one order of magnitude larger than those calculated on the basis of the reverse piezoelectric effect. It appears that crystal defects are largely responsible for the rather sizeable effects observed, thus preventing one from distinguishing field-dependent intrinsic contributions, such as those due to piezoelectricity and internal strains (Anastassakis, phys.stat.sol.(b) (1982) 110, 169).

11.5–5 X-RAY DIFFUSE SCATTERING IN LPE GaAlAs SOLID SOLUTIONS

C. Bocchi°, P. Franzosi° and C. Ghezzi°°

°Istituto MASPEC-CNR, Parma, Italy
°°Dipartimento di Fisica, Università di Parma, Italy

X-ray diffuse scattering (XRDS) experiments have been performed on thick (250 μm) $Ga_{1-x}Al_xAs$ (x=0.35±0.05) single crystal layers grown on (100) GaAs crystals by the liquid phase epitaxy (LPE). Using monochromatized Cu Kα radiation and small angular divergences (0.5°) of both the incident beam and the beam accepted by the counter, the I_D XRDS intensity has been accurately measured along the [100] direction in reciprocal space.
The intensity of the Compton scattering was independently measured at a few scattering angles by taking advantage of the energy resolution of a Si(Li) detector to partially separate the modified radiation. The Compton scattering data were interpolated by means of calculated incoherent scattering functions and then subtracted from the I_D. The I_{CW} intensity of the scattering due to composition waves is not dependent on the scattering vector $\vec{Q}$, while the I_{PH} intensity of the one-phonon scattering by LA and LO branches is proportional to Q^2. This made it possible to separate the two contribu-

tions to the I_D by comparing the XRDS intensity at equivalent points in reciprocal space. On the contrary, scattering contributions due to static displacements of the atoms were neglected, since they were evaluated as being on the order of a few 0.1% of the measured intensity.
As a result, the I_{CW} data were well fitted by the monotonic Von Laue scattering function $I_{CW} = (f_{Ga}-f_{Al})^2 x(1-x)$ with f_{Ga} and f_{Al} as scattering factors of Ga and Al atoms, respectively. This result shows that Ga and Al atoms, in LPE GaAlAs crystals, are distributed in the cation FCC sub-lattice in a completely random way. Moreover, the possibility of using XRDS experiments to investigate the atomic arrangement within the substituted sub-lattice in III-V solid solutions has been demonstrated. Recent investigations of phase separation and clustering criteria (see e.g. Stringfellow G.B., J. Electronic Materials 11, 903 (1982)) indicate that XRDS investigations on pseudobinary alloy semiconductors, such as InGaAs and InGaAsP, can be of great interest.

11.5–6 DEFECT STRUCTURE OF DEUTERIUM IN NIOBIUM - A NEW NEUTRON SCATTERING STUDY.
By H. Dosch, J. Peisl, Sektion Physik, Universität München, Germany; E. Burkel, Cornell University, Ithaca, N.Y. 14853, USA; B. Dorner ILL, Grenoble, France.

Detailed information on the location of deuterium, the long ranged displacement field and the local atomic distortions of the niobium lattice is deduced from measurements of the coherent elastic diffuse neutron scattering intensity distribution. Huang diffuse scattering (measured with D 10 of the ILL) confirms the cubic symmetry of the long ranging displacement field and the elastic force dipole tensor $P_{ij} = \delta_{ij}(3.32 \pm 0.05)$ eV.
The asymmetry of the scattering distribution leads to a location on tetrahedral sites. The scattering at large Q far away from Bragg reflections, the so-called "Zwischenreflex" - scattering (measured with IN2 of the ILL), cannot be explained by the model deduced from Huang diffuse scattering results. Model calculations which can explain both lead to a local defect structure, where lattice relaxation effects due to the rapid motion of deuterium in the lattice have to be taken into account. This also supplies an explanation for the cubic symmetry of the long ranged displacement field of a defect on tetrahedral sites.

11.6–1 X-RAY POLARIZATION BY BRAGG DIFFRACTION FROM BENT AND FLAT CRYSTALS.
By J. Zahrt, Chemistry Dept., Northern Arizona University, Flagstaff, AZ 86011, USA

Recently much attention has been given to the utilization of polarized X-rays in X-ray fluorescence spectrometers (R. Ryon, et.al., Adv. in X-Ray Anal., 25, 63 (1982)). The introduction of the extra scattering event to polarize the beam decreases the intensity. 90° scattering from the interior of a cylinder wall increases the intensity by utilizing a manifold of beams. This paper concerns itself with the development of a phenomenological theory, based on the mosaic model, to serve as a guide to developing better X-ray optics for Bragg scattered polarized X-ray spectrometers. The improved efficiency of the bent crystal (Johann) over the flat crystal has two sources. One is purely geometric and depends on the collimator(s) length ℓ, and radius τ, the radius of the Rowland circle R, and the displacement of the isotropic source from the Rowland circle e. The other source of improvement arises from the mosaic block size t, and from the mosaic distribution function here assumed to be Gaussian with standard deviation of $\eta/\sqrt{2}$. In the approximation of negligible true absorption and 1° and 2° extinction the theoretical results depend only upon geometry.

For Cu Kα diffraction from Cu(113) and ℓ=1cm, e=0.88cm, R=1.5cm and τ=0.15cm the reported efficiency ratio is bent/flat~3 (P. Wobrauschek, personal comm.). Using these parameters and t and η equal to 0.0001cm and 0.001 rad (flat) and 0.00005cm and 0.002 rad (bent) I calculate the ratio to be 3.3. Taking the t's 20 times larger and the η's 2 times larger gives 4.2. Taking ℓ=e=0 and the first set of crystal parameters gives 6.9.

I hope these results will be an aid in the construction of better spectrometers and encourage the determination of the mosaic parameters.

11.6–2 A TWO-CRYSTAL X-RAY INTERFEROMETER OF DIFFERENT SILICON MATERIALS.
By P. Becker, Physikalisch-Technische Bundesanstalt, Braunschweig, Federal Republic of Germany.

It has been shown that an X-ray interferometer consisting of two crystals cut from different silicon materials can be successfully operated. Experiments of this kind are of particular interest if lattice spacings of different crystals are to be measured on the meter scale, or if more space in the interfering beam paths is needed. Each of the two crystals shown in the figure belongs to a complete Laue-case interferometer tested separately in order to measure the homogeneity of the crystal lattice. The first crystal, bearing both the beam splitter S and the mirror M, was part of the scanning X-ray interferometer used for the absolute determination of the (220) lattice plane spacing (Becker, Dorenwendt, Ebeling, Lauer, Lucas, Probst, Rademacher, Reim, Seyfried, Siegert, Phys. Rev. Lett. (1981) 46, 1540). The second crystal with the analyzer A belongs to an interferometer cut in a similar way for the same purpose. The relative difference in the Bragg-plane spacings of the two silicon materials was about $(3 \pm 7) \times 10^{-8}$, measured by crystal-to-crystal comparison experiments (Becker, Seyfried, Siegert, Z. Phys. (1982) B 48, 17).

The geometrical deviations of the interferometer from the ideal shape caused by the manufacturing process are thoroughly investigated. In order to align the lattice planes of the two crystals parallel to one another by light optical means, the crystal surfaces are polished to form optical mirrors. Spacing marks are etched on the mirrors in order to realize equal distances between the three lamellas, S, M and A, by use of an optical length measuring device. Only a low interference contrast of $\approx$0.05 was observed in the outgoing beams. The reason for this is mainly the difference in thickness of more than 100 μm between the beam splitter S and the analyzer A.